CONTACT INTERACTION BETWEEN CORRUGATED STEEL SHELL AND THE SOIL BACKFILL DETERMINED BASED ON THE MEASUREMENTS OF SHELL DEFORMATIONS

C. MACHELSKI[1], L. KORUSIEWICZ[2]

Unlike in conventional bridges, the backfill and the roadway pavement have a major bearing on the load capacity of buried corrugated metal structures. In the soil-steel structure model one can distinguish two structural subsystems: the shell made of corrugated steel plates and the soil backfill with the road pavement. The interaction between them is modelled as a contact (interfacial) interaction, i.e. forces normal and tangent to the surface of the shell. The normal interactions are variable during both construction and service life. Two algorithms are presented. In the first algorithm on the basis of unit strains the internal forces in the shell are determined and consequently the contact interactions are calculated. A large number of measuring points distributed on the circumferential section of the shell is needed for the calculations. In the second algorithm the collocation condition, according to which the result obtained from the shell geometry model must agree with the measured displacement of the structure's collocation point, is used. When there are more such points, the estimated result is more precise. The advantage of both algorithms is that they take into account the physical characteristics of the soil in the backfill layers, but above all the backfill laying and compacting technology. The results of such analyses can be the basis for comparing the effectiveness of conventional geotechnical models.

Keywords: soil-shell structures, earth pressure, shell deformation, contact interaction

[1] Prof., DSc., PhD., Eng., Wrocław University of Science and Technology, Faculty of Civil Engineering, Wybrzeże Wyspiańskiego 27, 50-370 Wrocław, Poland, e-mail: czeslaw.machelski@pwr.edu.pl

[2] PhD., Eng., Wrocław University of Science and Technology, Faculty of Mechanical Engineering, Wybrzeże Wyspiańskiego 27, 50-370 Wrocław, Poland, e-mail: leszek.korusiewicz@pwr.edu.pl

1. INTRODUCTION

Understanding the distribution of soil pressure on buried structures is essential for the analysis and design of such constructions. Basic information about this aspect and the soil-structure interaction models for buried structures are presented in [1-3]. However, the geometric diversity of this type of structure often requires an individual approach to the discussed problem [4-11].

Additionally, the soil-structure interaction of a buried structure is affected by the material, size and stiffness; by the construction method; by the type and placement of the backfill material; and by the external loading [3, 4, 11-13]. Time-dependent analysis is described in [14, 15]. Many works concern the problem of adjusting the soil-steel interaction [9-11, 16, 17].

Currently, the assessment of the soil-structure interaction is most often conducted using numerical methods and verified on the basis of experimental data [4, 6, 7, 9, 11-13, 16, 18, 19]. Direct measurement of stress in the soil or the soil pressure on shell is possible using specially dedicated sensors [4, 8, 12, 15, 16, 18, 20, 21]. The reference of soil-structure interaction laboratory tests to the real conditions is discussed in [19, 22].

Although the relationship between the shell deformation and the soil pressure on its surface is commonly known, there is no description of detailed procedures allowing for calculation of contact interaction in the buried corrugated metal structures determined on the basis of the shell deformation measurements. That is why this paper concerns this problem.

The stiffness of a corrugated shell alone is small. During backfilling the shell deforms considerably as it is a geometric form confining the backfill during the bridge construction. As a result, during construction the shell carries the full soil pressure as if it was a retaining wall, but a flexible one. It is only when the shell is surrounded with backfill that it becomes an effective structural element capable of carrying considerable traffic loads. As opposed to conventional bridges, the characteristic feature of buried corrugated metal structures is the effect of the backfill and the roadway pavement acting as structural elements of a bridge [23]. The stiffness of soil-steel structures is comparable with that of conventional bridges (obviously the highest stiffness characterizes masonry bridges) [24].

In models of soil-steel structures two structural subsystems can be distinguished: the shell made of corrugated plates and the other part consisting of the backfill and the road pavement. The interaction between the two subsystems is modelled as contact interaction in the form of surface forces: normal force p and tangential force t, as shown in Fig.1. In order to render soil-steel structure performance in FEM models on the basis of shell strain measurements the following two groups of results are used:

- strains in corrugated plate cross sections to determine internal forces in shell measurement points;

- point displacements determining the shape of the shell buried in soil.

It should be pointed out that the instrumentation layout is very important to get results that can be used for purpose of calibration FEM model simulations.

The effectiveness of the two ways of determining the action of the soil on the shell is compared in this paper. The two ways differ in their methodologies of determining contact interaction, but the shell deformation measurements are used in both cases. Therefore, the main aim of this paper is to indicate the possibility of analysing contact interaction using classical measurement techniques: strain gauges and geodetic measurements. One of the examples provided in the paper concerns the construction phase, and the second one the exploitation phase. Separate calculation methodologies are used for each of these cases.

The shell's upper part with curvature radius R is analysed. This part of the shell is subjected to the strongest live loads influence. The effects of the soil pressure on the shell occurring during bridge construction and exploitation can be summed. Therefore a FEM model used to analyse the forces in the soil medium must take into account the state which existed during bridge construction.

Determination of the soil pressure on the shell is a non-conventional geotechnical problem. For the surcharge load in a form of a concentrated force, it becomes the Boussinesq problem. When the effect of the backfill dead load (distributed surcharge load) is considered, the classical Coulomb, Müller-Breslau and Rankin solutions apply. The methods of: Duncan, Spangler, White and Layer, Meyerhof and Baike, Klöppel and Glöck, and many other, have been used to design corrugated shells. In many works (e.g. [15, 25-28]) attempts have been undertaken to determine the soil pressure on the shell by means of various methods.
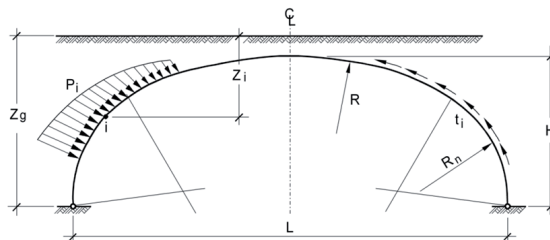

Fig. 1. Diagram of shell's circumferential section and contact forces

2. SHELL PLATE STRAIN − SOIL PRESSURE DEPENDENCE

The set of electrical resistance strain gauges, shown in Fig. 2, is used to determine internal forces on the basis of shell deformations. Electrical resistance strain gauges are glued to the corrugated shell inside surface in a circumferential section of the structure. Two gauges are placed – one in the corrugation's crest (strain ε_D) and the other in its valley (strain ε_g) – in each measuring point along the circumferential section. It is useful to adopt regular spacing between the strain gauges when using the finite difference method in calculations.
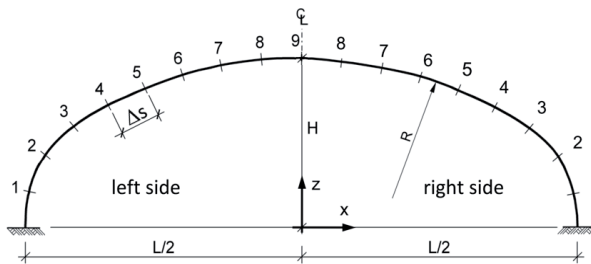
Fig. 2. Arrangement of strain gauges on shell's circumferential section

As an example of extensiometric investigations this paper presents results of measurements carried out on a soil-steel structure during its construction [23, 24]. This road soil-steel structure is located in Ostróda (Poland) and has a record-breaking span. The geometric design parameters of the shell's circumferential section, on the axis of inertia of the corrugated plate are as follows: span $L = 25.751$ m, height $H = 9.116$ m and radius of curvature in crown $R = 16.636$ m and in shoulder $R_n = 6.12$ m. The structure's largest geometric parameter is its length, amounting to 95.70 m at the base and to 67.52 m in the crown. The corrugation profile of this structure is known as UltraCor, which is designated under CAN/CSA-G401-14 as Type III corrugation and under CAN/CSA-S6-14 as deeper corrugation. The corrugation profile is UC $a \times f \times t$, i.e. UC 500×237×9.65 mm (where: a –the length of the corrugation, f – the height of the corrugation, t – the thickness of the plate). The mechanical properties per mill certification are $F_y = 478$ MPa and $F_u = 585$ MPa. The structure was subjected to tests described in [29].

Thanks to the twin arrangement of the strain gauges it was possible to determine the strains on the axis of inertia of the cross section (assuming the latter to be flat) of the corrugated plate from the relation (symbols as in Fig. 3)

(2,1)
$$\varepsilon = \frac{\varepsilon_D(f - t) + \varepsilon_g(f + t)}{2f}$$

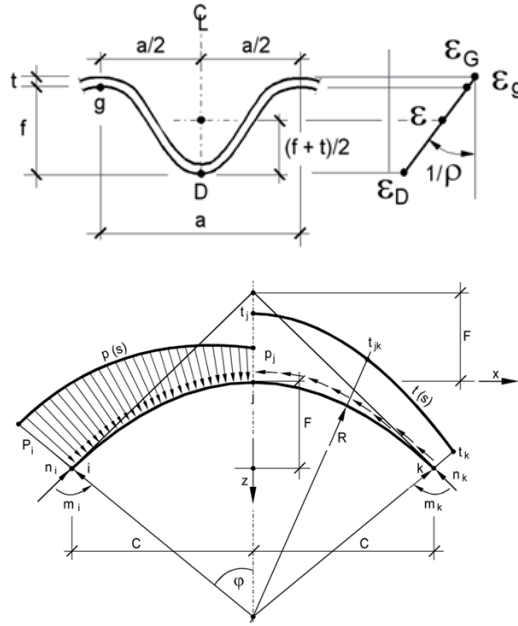
Fig. 3. Denotations of internal forces, contact interactions and shell strains

Formula (2.1) takes into account the geometry of corrugated plate UC $a \times f \times t$. In order to determine the change in the shell curvature radius one can use the plate's geometrical dependences and ε_D and ε_g as in the equation

(2.2)
$$\frac{1}{\rho} = \frac{\varepsilon_D - \varepsilon_g}{f}$$

The geometric quantities calculated from Eq. (2.1) and Eq. (2.2) are used to determine the internal forces in the shell, i.e. the axial force

(2.3)
$$n = \frac{E \cdot A}{a} \varepsilon$$

and the bending moment

(2.4)
$$m = \frac{E \cdot I}{a} \frac{1}{\rho}$$

where: $A/a = 14.51$ mm^2/mm and $I/a = 96766$ mm^4/mm are the cross sectional geometric characteristics of the corrugated plate (with corrugation length a) and $E = 205000$ MPa is the Young's modulus of the material (steel).

The general relations that connect the internal forces in the shell with the considered contact interactions have the following form

$$(2.5) \qquad p = \frac{d^2 m}{ds^2} + \frac{n}{R}$$

$$(2.6) \qquad t = \frac{dn}{ds} + \frac{1}{R}\frac{dm}{ds}$$

In equations (2.5) and (2.6), s is counted along the perimeter band of the shell with a radius R. In the case of a regular system of measuring points (Fig. 2), it is convenient to use a differential approach to determine the contact forces.

From static internal forces n and m (calculated from formulas (2.3) and (2.4)) as a function of the distance between points, but along the circumferential section one gets (in differential terms) the normal interactions

$$(2.7) \qquad p_j = \frac{m_i - 2m_j + m_k}{(\Delta s)^2} + \frac{n_j}{R}$$

and the tangential interactions

$$(2.8) \qquad t_{jk} = \frac{n_j - n_k}{\Delta s} + \frac{m_j - m_k}{\Delta s \cdot R}$$

The value of p_j is calculated in shell measuring point j while that of force t_{jk} between points j and k, as in Fig. 3. In the case of a dense arrangement of points on the arc, the arc length between the measuring points is nearly similar to the length of segment Δs (as in Fig. 2), because angle φ (Fig. 3) is small and is equal to about 6°. In the case when the arc length between adjacent points j is different than Δs, equation (2.7) takes the following form

$$(2.9) \qquad p_j = \frac{2}{(\Delta s)^2(1 + \alpha)\alpha}\left[\alpha \cdot m_i - (1 + \alpha)m_j + m_k\right] + \frac{n_j}{R}$$

where $\Delta s = \Delta s_{ij}$ and $\alpha = \Delta s_{jk} / \Delta s_{ij}$.

The differential equations are derived from the geometrical relationships for the peripheral band of the shell with one radius of curvature R. Thus, the band is considered as a bar with the shape given in Figure 2. The interval between the measuring points has a significant effect on the calculation result in the case of complex functions $\varepsilon(s)$. If the function between points i, j and k is close to the second-order parabola, a very good approximation is obtained as shown below.

3. EXAMPLE OF CONTACT INTERACTIONS DURING CONSTRUCTION

The results of investigations of the considered structure, in the form of diagrams of strains ε and internal forces m and n for different backfill levels z_g (as in Fig. 1) were presented in [24]. Figure 4 shows contact interactions, in the form of normal components p and tangential components t, determined for the final construction phase (when $z_g = 11.8$ m). The values of s – the distance of the considered cross section from the shell crown, calculated along the shell circumferential section (when $s = 0$, the measuring point is located on the structure's symmetry axis, as in Fig. 2, point 9), are marked on the horizontal axis of the diagrams. Thus the distances between the measuring points on the left side of the shell are negative, amounting to

$$(3.1) \qquad\qquad -s_i = 2.25 + 2.0(8 - i) \quad [\text{m}]$$

when $i < 9$ is the number of the measuring point, as in Fig. 2. In the figures mentioned in this section negative values of s represent the left side of the arch while positive values of s represent the right side of the arch.

Since the shell's upper part, where the curvature radius is constant and equal to R, is considered, the location of any point can be determined using the angular measure, as
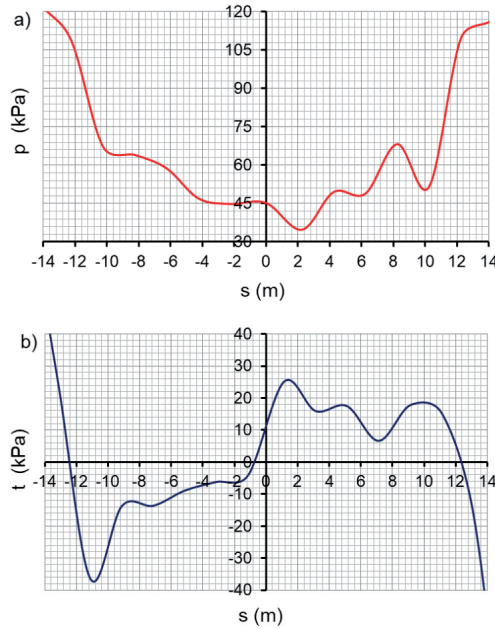
$$(3.2) \qquad\qquad \varphi = \frac{s}{R}$$

Fig. 4. Soil pressure along shell's circumferential section length $z_g = 11.8$ m: a) normal components p, b) tangential components t

The backfill level is measured from the foundation, as z_g. In the diagram (Fig. 5) it is related to shell height H. Hence the location of the considered point relative to the foundation can be determined as follows

$$(3.3) \qquad\qquad z = H - F = H - R(1 - \cos \varphi_0)$$

when φ from formula (3.2) is converted into degrees, denoted as φ_0.

From the above geometric relations one determines the locations of the measuring points, but in the x, z coordinate system as in Table 1. The locations of the points in which contact interactions are calculated are given in Table 2. It appears from the results shown in Table 2 that the lowest analysed point in Fig. 5 is consistent with measuring point 4 and backfill level $z_g/H = 0.68$.
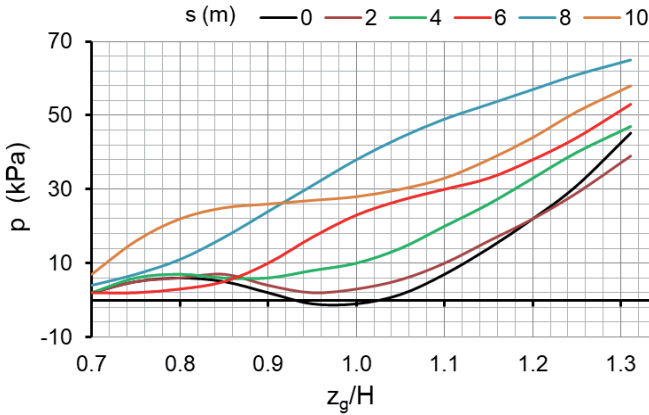
Fig. 5. Changes in soil pressure in circumferential section of shell

Table 1. Locations of measuring points on shell's circumferential section

Location parameter	Measuring points as in Fig. 2					
	9	8	7	6	5	4
s (m)	0	2.25	4.25	6.25	8.25	10.25
z/H	1	0.983	0.943	0.971	0.776	0.679
φ_o (°)	0	7.75	14.64	21.53	28.42	35.31

Table 2. Parameters of location of calculation points on shell's circumferential section

φ	0	0.1	0.2	0.3	0.4	0.5	0.6
s (m)	0	1.66	3.33	4.99	6.65	8.32	9.98
z/H	1	0.990	0.963	0.918	0.855	0.773	0.678
φ_o (°)	0	5.72	11.44	17.16	22.87	28.59	34.31

The results presented in Fig. 5 were obtained on the basis of Fig. 4a, as averages taken from the left side and the right side jointly since the system is nearly symmetric. The shape of the tangential forces shown in Fig. 4b is nearly asymmetric. Figure 5 shows graphs of the pressure exerted on the shell points specified by angular measure φ according to equation (3.2) and the data contained in Table 2. Backfill levels related to shell height H (when $z_g/H = 1$, the backfill reaches the shell crown level) are marked on the horizontal axis. The values of p in Fig. 4a at $z_g/H = 1.311$ indicate a moderately uniform distribution of soil pressure along the whole length of the circumferential section of the shell.

The graphs in Fig. 5 show that the values of p are low when the backfill level is lower than the considered shell point. According to the static load calculation assumptions, when the soil level is below the considered shell point, no contact interaction should occur. Therefore it follows from equation (2.5) that the following relation should be satisfied

$$(3.4) \qquad\qquad R\frac{d^2m}{ds^2} = -n$$

In neighbouring points j and k the following relation should hold true

$$(3.5) \qquad\qquad R(n_j - n_k) = m_k - m_j$$

In the case of in-situ testing, as in this paper, climate conditions affect measurement results. A part of the shell is embedded in the soil medium while the middle part protruding from the soil is exposed to temperature changes, wind and humidity. In such situations small deviations from $p = 0$ (Fig. 5) may also be due to the measuring methodology.

Figure 6 shows contact interaction diagrams for the special case when the backfill level reaches the crown of the shell, i.e. when $z_g = H$.
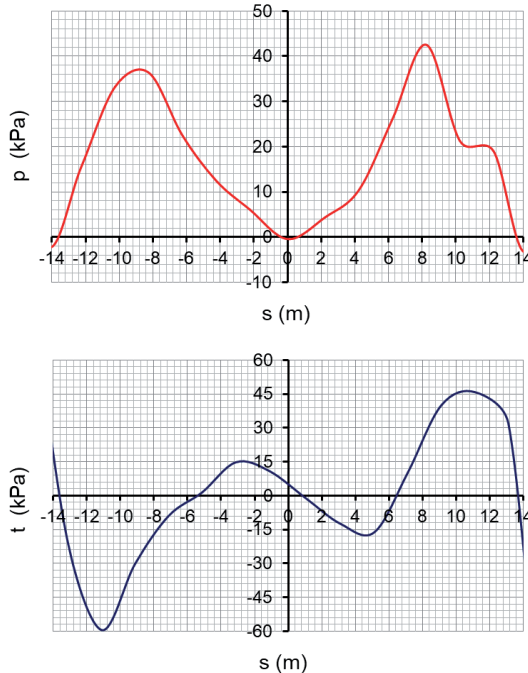

Fig. 6. Soil pressures along shell's circumferential section length $z_g = H$

The graph of p values indicates exceptionally good agreement with the remarks made earlier since p ≈ 0 when s = 0. When s ≈ 9 m, function $p(s)$ reaches its maximum and when s = 14 m, pressures p are reduced to zero. An analysis of the other diagrams shows that when $z_g < H$, soil pressures p in the shell crown area are usually small. This is connected with a reduction in the curvature radius from R = 16.632 m to R_n = 6.12 m between points 3 and 4. According to Figure 2, the change in the curvature radius occurs at distance s ≈ 11.25 m from the crown. A clear increase in soil pressure in this area is observed when soil surcharge is being formed, i.e. when the backfill level is higher than the shell crown, and its maximum value is as in Fig. 4. The graph of $t(s)$ is usually asymmetric relative to the vertical axis (when s = 0) and the values of t are usually lower than p.

A very good effectiveness of the presented algorithm results from the shape of the structure, and especially from the regular functions $m(s)$ and $n(s)$, which are also calculated using regular functions $ε(s)$. In the case of the similar algorithm used in [30], it was necessary to use a special procedure of "smoothing" the input data.

The presented algorithm was also used to analyse the effects of service (test) loads [31, 32]. The tests were carried out using the same measurement base of the structure that was analysed in the paper. The results of calculations in the form of displacements, which were obtained from strain gauge measurements and the algorithm given in the paper, were compared with the measurements of inductive sensors, as well as geodetic measurements. They indicated a good compatibility.

4. SHELL DISPLACEMENT − SOIL PRESSURE DEPENDENCE

By dividing the soil-steel structure in two structural subsystems one can independently analyse the shell subjected to an external load in the form of contact forces with components p and t. The forces are exerted on the shell by the backfill (the second subsystem). The corrugated shell is an ideal model of an elastic system with bending stiffness EI/a and axial-force stiffness EA/a. Then a 2D model, as in Fig. 7, is used for the calculations.
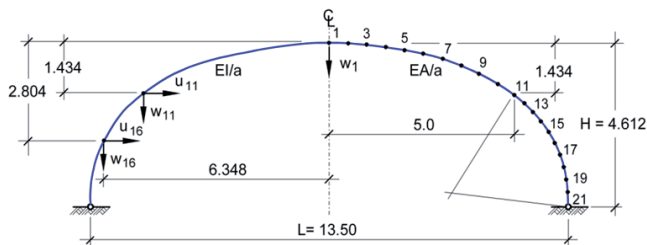

Fig. 7. Model for calculating shell and displacement of collocation points

In this paper a collocation condition is used to determine the interaction between the two subsystems. In order to satisfy this condition the measured displacement of the structure's collocation point, denoted as r, must agree with the calculation result obtained using the shell geometry model, as follows

(4.1)
$$r = \mathbf{f_{rp}} \cdot \mathbf{p}$$

Thus the measurement result and the shell deformation are on the left side of equation (4.1) while the displacement result calculated using the model is on the right side of the equation. In formula (4.1) $\mathbf{p}$ is the vector of the force (the normal component of the soil pressure exerted on the shell) uniformly distributed on the shell's circumferential section. The values of vector $\mathbf{p}$ are determined in the nodes of the division of the shell into elements, as in Figs 1 and 3. The vector has this form

(4.2)
$$\mathbf{p} = \text{col}\{p_1,\ p_2,\ p_3, \ldots \ldots p_i, \ldots \ldots p_n\}$$

Vector $\mathbf{f_{rp}}$ is an influence function of displacement r caused by normal components of vector $\mathbf{p}$

(4.3)
$$\mathbf{f_{rp}} = \{f_1,\ f_2,\ f_3, \ldots \ldots f_i, \ldots \ldots f_n\}$$

Tangential components $t(s)$ and normal components $p(s)$ of the interaction are mutually confounded through the coefficient of friction. The effect of the tangential component on displacements (which are usually small) is disregarded in the considerations and in the results of measurements.

The presented algorithm assumes the symmetry of the deformation of the shell, and thus of the contact interactions. For this reason, half of the circumferential section of the shell is considered in the 2D model. The terms f_i of the influence function vector are defined as the result of the calculations obtained from the model given in Figure 7 (on the right) from the unit loads ($p = 1$) of particular nodes, and therefore there is a concentrated force with the radial direction $P_j = p \times \Delta s$, where Δs is the arc length between the points (constant value). Thus, the value f_j is the displacement of the analysed point j due to load P_j.

The form of solution (4.1) shows that for each considered displacement r, the terms of the influence function will obtain a different value. The calculated terms p_i of the pressure vector are also differentiated, as in the examples given in the paper.

The form of equation (4.1) and formulas (4.2) and (4.3) indicates the drawback of the proposed analytical methodology. In mathematics this drawback is called solution nonuniqueness. It is due to the fact that a considerable number of terms p_i is determined on the basis of a single value of r and collocation condition (4.1). The method of successive approximations is used to obtain reliable estimates of the function of interactions **p** in equation (4.1). The values p_i are more precise when several collocation conditions, i.e. displacements of points r, are used (as in the example provided in this paper). Therefore the Müller-Breslau solution [33] can be useful for the first approximation. The solution has the form of the static soil pressure

(4.4) $$p_i = \gamma_g \cdot K_a \cdot z_i - 2c\sqrt{K_a}$$

where: γ_g – the weight density of the soil and c – the coefficient of cohesion. The pressure distribution in (4.4) linearly depends on backfill depth z_i (the distance of the considered point from the soil surcharge level, as in Fig. 1). The shape of the shell and the parameters of the soil are taken into account as the function of many variables: $K_a(\alpha, \beta, \varphi, \delta)$ [33].

It should be noted that relation (4.4) is for the soil pressure exerted on solid retaining walls, not on a slender corrugated shell, as in this paper. The discrepancies between the results yielded by the algorithm and the p_i values obtained from (4.4) can be considerable since the values of p_i calculated from (4.1) take into account the actual physical parameters of the backfill and its layered system whose physical characteristics vary due to the different degrees of soil compaction and sometimes to the different kinds of soil. An important factor is the backfilling method. The first subsystem's static characteristics, such as the shape of the shell and its stiffness distribution (taken into account in the terms of displacement influence components f_i (mm/kPa) of vector **f**$_{rp}$), are a solid basis for relation (4.3).

In [34], the discussed algorithm was used to determine the displacement r of the shell, but this time due to the backfill being loaded with a car. In this case, the influence functions that are obtained from the tests, and those that were obtained from calculations using the 2D model and the PLAXIS software, were compared.

5. ANALYSIS OF SOIL PRESSURE VERSUS TIME

Figure 1 shows the cross sectional shape of a built typical soil-steel structure denoted as SC-15NA [35]. The conduit profile is a two radius arch with span $L = 13.50$ m and height $H = 4.68$ m and the soil surcharge is 3.72 m thick. The shell is made of SC 381×130×7 corrugated plates. The deformations measured during construction and service life indicate that the shell is nearly symmetrical, which was taken into account in the calculation model shown in Fig. 7. The pressures exerted on the shell by the backfill are estimated on the basis of the measured displacements of points located on the shell, as on the left side of Fig. 7. From among the measuring points the following are distinguished: the point in the shell crown and the two twin points on its side wall [35].

Figure 8 shows changes in the displacements of the measuring points recorded during the construction (1-67-107 days) and use of the structure (for over 6 years). It appears from the graphs that the dominant displacement values characterize w_1, u_{11} and u_{16}. In this paper the above displacements were used as the values of r in collocation condition (4.1).

Figure 9 shows the influence functions of selected displacements for the case when the load is a force uniformly distributed on two segments between points $i − 1$ and $i + 1$ (the force is assigned to considered point i). It appears from the graphs that displacements w_1 and u_{11} as well as u_{16} are useful for determining pressures p_i. Since influence function $f(w_1)$ is essential for determining pressure p_i exerted on the shell crown, it can be assumed as the basic one. It appears from graphs $f(u_{11})$ and $f(u_{16})$ that even small changes in p_i significantly affect the horizontal displacements in the shell's haunch. The possibilities of using function $f(w_{11})$ as the collocation condition are limited, which is also reflected in the values shown in Fig. 8.
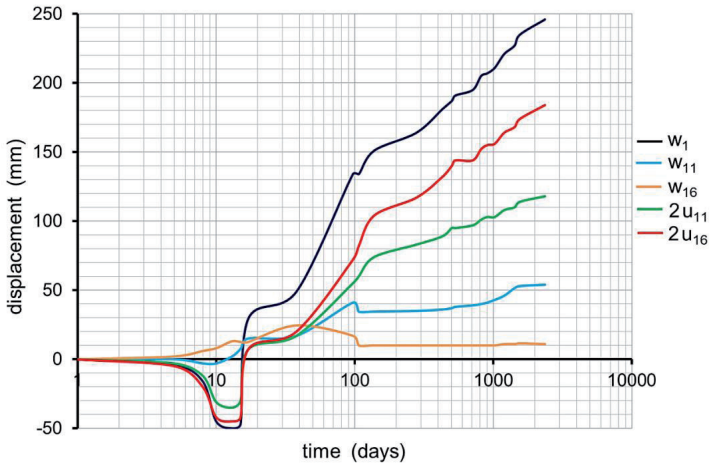
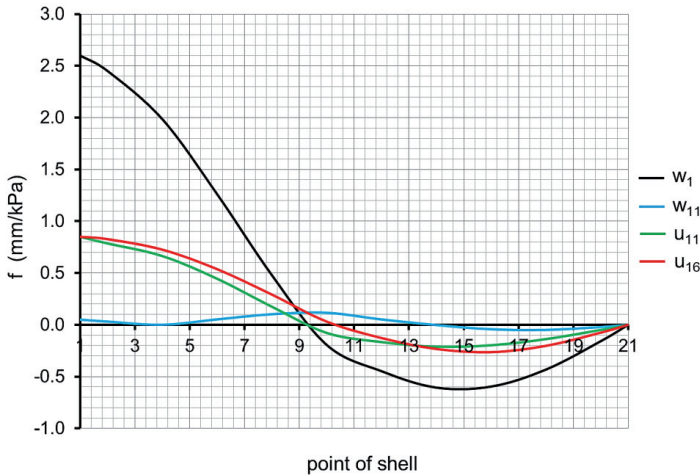Fig. 8. Changes in displacements of shell points during construction and service life

Fig. 9. Influence functions of shell displacements

The normal components of forces p_i acting on the shell were determined in three construction phases (1-107 days) and in three service life intervals (107-2364 days). Table 3 shows the measured displacements of the measuring points, as in Fig. 8, used to calculate p_i. The last column shows the soil pressure values in support point 21 (the concrete wall supporting the shell) calculated from formula (4.4), assuming $c = 0$ and as the constant: $\gamma_g \times K_a = 12$ kN/m^3, hence $p_{21} = 12 \times z_g$.

Laboratory tests carried out on samples of backfill soil taken from the structure showed an exceptionally high value of γ_g – 23.5 kN/m^3.

Table 3. Changes in displacements and interactions during construction and service life of soil-steel structure

Measurement time (days)		Displacements of points (mm)			Interaction	
		w_1	u_{11}	u_{16}	z_g (m)	p_{21} (kPa)
construction	13	-50	-17.5	-22.5	4.7	56.4
	38	49	8.5	10	6.5	78.0
	107	134	30	41		
service	107	134	30	41	8.4	100.8
	1200	221	54	82		
	2364	246	59	92		

Figure 10 shows soil pressures p_i calculated from condition (4.1) when $r = w_1$, i.e. on the basis of the deflection of the shell crown. The graphs shown in Fig. 11 were obtained in a similar way, but using horizontal displacement u_{11}. In Figure 12 the horizontal displacement (u_{16}) of the shell side wall was assumed as the collocation condition. Since each of the collocation conditions is considered independently, different distributions of forces $p(s)$ (shown in Figs 10-12) are obtained. The main aim of the investigations was to compare the graphs obtained for the same time intervals during the service life of the structure. Considering that despite the change of the collocation condition the difference between the graphs is small, one can say that pressures $p(s)$ were accurately estimated.
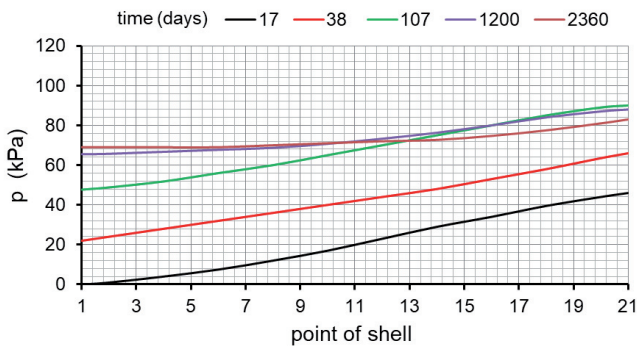

Fig. 10. Changes in soil pressure calculated from collocation condition $r = w_1$
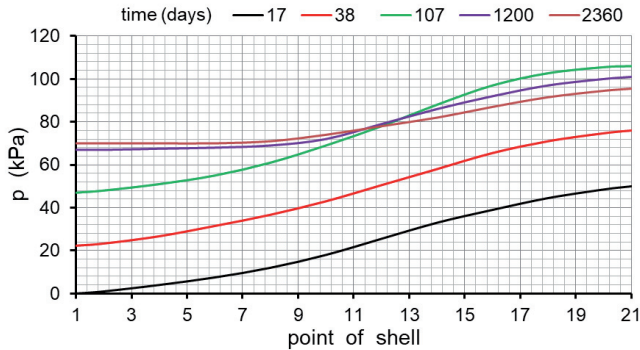
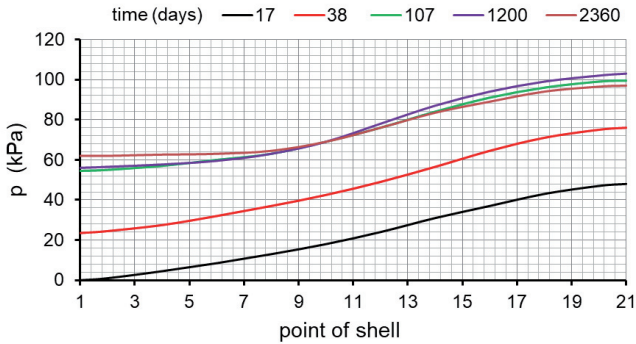Fig. 11. Changes in soil pressure calculated from collocation condition $r = u_{11}$

Fig. 12. Changes in soil pressure calculated from collocation condition $r = u_{16}$

Equation (4.1), but applied to the other measuring points of the shell, is used to verify the estimated soil pressures. Table 4 shows (in bold) the results of such calculations for two of the remaining collocation points, based on the collocation point displacement given in Tab. 3. A comparison of the displacement values contained in Tables 3 and 4 shows considerable differences between them despite the fact that the changes in function $p(s)$ are small, which corroborates the earlier conclusion. Also the assumption about model symmetry and the form of deformation, on which the investigation methodology in [35] was based, has a bearing on the discrepancies between the results. The effect of tangential forces t_i was not taken into account in the algorithm.

The graphs in Figs 10-12 are presented mainly to demonstrate the effectiveness of estimating changes in the soil pressures exerted on the shell when shell displacements continue to propagate, as shown in Fig. 8.

Tab. 4. Calculated displacements of shell measuring points

Measurement time (days)		Displacements of points (mm)		
		w_1	u_{11}	u_{16}
construction	13	**-50**	-16.70	-18.16
		-52.72	**-17,5**	-19.25
		-59.41	-20.09	**-22,5**
	38	**49**	15.84	21.84
		27.34	**8,5**	13.12
		19.81	6.09	**10**
	107	**134**	26.22	56.20
		144.12	**30**	59.51
		96.98	13.80	**41**
service	1200	**221**	81.08	89.62
		142.0	**54**	58.41
		203.0	74.93	**82**
	2364	**246**	80.69	99.28
		179.64	**59**	72.65
		227.50	74.55	**92**

6. CONCLUSIONS

Using the results of measurements performed on the actual structure (3D) the calculation model is reduced to planar (2D) systems. The shell's deformations, defined by the displacements of measuring points, in the form of vertical components w and horizontal components u, are used to determine contact interactions: pressures p and tangential forces t. The displacements are measured using geodetic techniques, which are sufficiently precise because of the high displacement values. Contact interactions can also be determined through internal forces calculated from the shell's deformations, but the latter are measured in many points on the circumferential section by means of strain gauges (this means that they are unit strains). So the measuring methodology is different than in the case above.

The results yielded by the two methods are verified through the direct measurement of soil pressure by means of a pressure meter. This way of measuring interferes directly in the soil-shell interfacial layer. Both the solutions considered in this paper use the soil-shell interaction consistency condition.

No consistency condition for displacements in the interfacial layer is taken into account, which means that the occurrence of slip between the two subsystems is permitted. This is an important advantage of the algorithm.

Knowing contact interactions p and t one can analyse each of the subsystems (the corrugated shell and the backfill + the pavement) separately. The contact interactions can be used to analyse the internal forces and the displacements of the soil medium as the second subsystem. It is difficult to model the soil because of its complex layered structure and the individual characteristics of each of the layers. It is very difficult to determine soil displacements on the basis of the deformation of the shell in the interfacial layer since slips can arise in the plate-soil interface.

Two different algorithms for calculating contact interactions have been presented. In the first algorithm on the basis of unit strains the internal forces in the shell are determined and consequently the contact interactions are calculated. A large number of measuring points distributed on the circumferential section of the shell is needed for the calculations. In the second algorithm the collocation condition, according to which the result obtained from the shell geometry model must agree with the measured displacement of the structure's collocation point, is used. In this case, a small number of points is sufficient. When there are more such points the estimated result is more precise. The advantage of both algorithms is that they take into account the physical characteristics of the soil in the backfill layers, but above all the backfill laying and compacting technology. Soil-steel structures are analysed when they are under construction (during backfilling) and in service (with the completed surcharge and the roadway). No road or rail vehicle loads are taken into account in the calculations. In the case of soil-steel structures, the impacts of live (moving) loads are a separate problem [28, 29, 34, 36-38].

The analysis of contact forces can be used for the modelling of the interface in FEM software (PLAXIS, ABACUS). The interface model should, however, be different during the construction phase (laying up the backfill), different for service loads (passage of vehicles), and also different when referring to the effects of operation (as long-term processes).

It is particularly important to observe the changes in p and t interactions during operation. The second algorithm, using the geodetic equipment with a small number of measuring points, may be used to observe these changes (as shown in the example given in Figures 8-12).

The two presented algorithms for observing changes in the soil impact on the shell can successfully replace more complicated and more expensive measurements that use earth pressure cells.

REFERENCES

1. T.J. McGrath, "Development of design and analysis methods for buried culverts", Transportation Research Circular, Number E-C230, 1-12, March 2018.
2. M.G. Katona, "History of soil–structure interaction models for buried culverts", Transportation Research Circular, Number E-C230, 13-20, March 2018.
3. T.C. Sandford, "Soil-structure interaction of buried structures", Transportation in the New Millennium, TRB, 2000.
4. O. Abuhajar, M.H. El Naggar, T. Newson, "Comparison of soil pressure measurements around square box culverts using different techniques", Conference Paper: 69th Canadian Geotechnical Conference, Vancouver, BC, Canada, October 2016.
5. J. Kang, F. Parker, C.H. Yoo, "Soil–structure interaction for deeply buried corrugated steel pipes. Part I: Embankment installation", Engineering Structures 30(2): 384-392, 2008.
6. M.X. Zhang, B.D. Liu, P.F. Li, Z.M. Feng, "Structure-soil interaction of buried corrugated steel arch bridge", Advanced Materials Research 163-167: 2112-2117, 2011.
7. M. Kumar, M.D. Goel, V.A. Matsagar, K.S. Rao, "Response of semi-buried structures subjected to multiple blast loading considering soil–structure interaction", Indian Geotechnical Journal 45(3): 243-253, 2015.
8. A.M. Abdel-Karim, M.K. Tadros, J.V. Benak, "Structural response of full-scale concrete box culvert", Journal of Structural Engineering 119(11): 3238-3254, 1993.
9. J. Kang, F. Parker, C.H. Yoo, "Soil-structure interaction and imperfect trench installations for deeply buried corrugated polyvinyl chloride pipes", Transportation Research Record: Journal of the Transportation Research Board 2028 (1): 192-202, 2007.
10. W.S. Yu, Z.L. Li, X.R. Xie, L.Y. Guo, "Experimental study on earth pressure of corrugated steel culvert under high fill embankment", Applied Mechanics and Materials 405-408: 1815-1819, 2013.
11. E. Bayoğlu Flener, "Soil-steel interaction of long-span box culverts−performance during backfilling", Journal of Geotechnical and Geoenvironmental Engineering 136(6): 823-832, 2010.
12. B. Liu, Z. Wang, W. Xu, H. Sun, X. Wang, "Comparative experimental study and FE analysis of corrugated steel pipe culverts with different stiffness", The Open Civil Engineering Journal 10: 549-563, 2016.
13. B. Liu, M. Zhang, P. Li, Z. Feng, "Effect of parameters on soil-structure interaction of a buried corrugated steel arch bridge", The Open Civil Engineering Journal 5: 154-162, 2011.
14. M. McVay, P. Papadopoulos, "Long term behavior of buried large-span culverts", Journal of Geotechnical Engineering 112(4): 424-442, 1986.
15. J. Vaslestad, B. Kunecki, T.H. Johansen, "Twenty one years of earth pressure measurements on buried flexible steel structure", Archiwum Instytutu Inżynierii Lądowej/Archives of Institute of Civil Engineering (1): 233-244, 2007.
16. M.R. Ahmed, V.D.H. Tran, M.A. Meguid, "On the role of geogrid reinforcement in reducing earth pressure on buried pipes: experimental and numerical investigations", Soils and Foundations 55(3): 588–599, 2015.
17. J. Kang, F. Parker, C.H. Yoo, "Soil–structure interaction for deeply buried corrugated steel pipes. Part II: Imperfect trench installation", Engineering Structures 30(3): 588–594, 2008.
18. B. Kunecki, "Full-scale test of corrugated steel culvert and FEM analysis with various static systems", Studia Geotechnica et Mechanica 28(2): 39-54, 2006.
19. L. Korusiewicz, B. Kunecki, "On boundary conditions in experimental and numerical models of steel culverts", in: W. Pietraszkiewicz, C. Szymczak (Eds.), Shell Structures: Theory and Applications, Taylor & Francis Group, London, 573-576, 2005.
20. M.C. Palmer, T.D. O'Rourke, N.A. Olson, T. Abdoun, D. Ha, M.J. O'Rourke, "Tactile Pressure Sensors for Soil-Structure Interaction Assessment", Journal of Geotechnical and Geoenvironmental Engineering 135(11): 1638–1645, 2009.
21. M.L. Talesnick, H.-W. Xia, I.D. Moore, "Earth pressure measurements on buried HDPE pipe", Geotechnique 61(9): 721-732, 2011.
22. R.W.I. Brachman, I.D. Moore, R.K. Rowe, "The design of a laboratory facility for evaluating the structural response of small-diameter buried pipes", Canadian Geotechnical Journal 37(2): 281-295, 2000.
23. C. Machelski, L. Janusz, P. Tomala, K. Wiliams, "Deformation parameters of deep corrugated soil-steel structures", in: Transportation Research Board 97th Annual Meeting, Washington DC, United States, 2018, Paper Number: 18-05399.
24. B. Kunecki, L. Janusz, L. Korusiewicz, K. Wiliams, "Field tests of deep corrugated super-span metal arch during backfilling", in: Transportation Research Board 97th Annual Meeting, Washington DC, United States, 2018, Paper Number: 18-03926.
25. B. Bakht, "Evaluations of the design methods for soil-steel structures in Canada", Archiwum Instytutu Inżynierii Lądowej/Archives of Institute of Civil Engineering (1): 7-22, 2007.

26. W.S. Szajna, "Numerical model for the analysis of construction process of soil-steel culverts", Archiwum Instytutu Inżynierii Lądowej/Archives of Institute of Civil Engineering (1): 215-223, 2007.
27. C. Machelski, "Estimation of internal forces in the shell of soil-steel structures on the basis of its displacements during backfilling", Studia Geotechnica et Mechanica 31(1): 19−38, 2009.
28. C. Machelski, "Kinematic method for determining influence function of internal forces in the steel shell of soil-steel bridge", Studia Geotechnica et Mechanica 32(3): 27−40, 2010.
29. C. Machelski, "Dependence of deformation of soil-shell structure on the direction of load passage", Roads and Bridges 13(3): 223−233, 2014.
30. C. Machelski, "Dead load effect of bridges constructed with cantilever concreting technology", Architecture Civil Engineering Environment 12(1): 109-120, 2019.
31. C. Machelski, "Soil–steel structure shell displacement functions based on tensometric measurements", Studia Geotechnica et Mechanica 40(3): 170-179, 2018.
32. C. Machelski, P. Tomala, "Investigation of displacements function in soil-steel bridge based on strain gauges measurements". in: Steel Bridges, 9th International Symposium on Steel Bridges, Czech Constructional Steelwork Association, European Convention for Constructional Steelwork, Prague, 1-18, 2018.
33. H. Müller-Breslau, "Erddruck auf Stützmauern", Alfred Kröner Verlag, Stuttgart, 1906 (in German)
34. C. Machelski, L. Janusz, "Application of results of tests in developing a two-dimensional model for soil-steel railway bridges", Transportation Research Record: Journal of the Transportation Research Board 2656(1): 53−60, 2017.
35. C. Machelski, "Estimation of the interaction effects of backfill on the shell in the soil-steel structure based on deformation of the shell", Przegląd Komunikacyjny 71(11): 31-36, 2016.
36. M. L. Silver, H. B. Seed, "Volume Changes in Sands during Cyclic Loading", Journal of the Soil Mechanics and Foundations Division 97(9): 1171-1182, 1971.
37. M. Sobótka, "Numerical simulation of hysteretic live load effect in soil-steel bridge", Studia Geotechnica et Mechanica 36(1): 103−109, 2014.
38. K. White, S. Sargand, T. Massada, "Evaluation of load rating procedure for metal culverts under shallow soil covers", Archiwum Instytutu Inżynierii Lądowej / Archives of Institute of Civil Engineering (23): 311-323, 2017.

LIST OF FIGURES AND TABLES:

ODDZIAŁYWANIE KONTAKTOWE MIĘDZY POWŁOKĄ ZE STALI FALISTEJ A ZASYPKĄ GRUNTOWĄ OKREŚLONE NA PODSTAWIE POMIARÓW ODKSZTAŁCEŃ POWŁOKI

Słowa kluczowe: konstrukcje gruntowo-powłokowe, napór gruntu, deformacja powłoki, oddziaływanie kontaktowe

STRESZCZENIE:

Charakterystyczną cechą konstrukcji gruntowo-powłokowych, w odróżnieniu od klasycznych mostów, jest duży wpływ zasypki gruntowej i nawierzchni jezdni jako elementów nośnych obiektu. W modelu obiektu gruntowo-powłokowego wyróżnia się dwa podukłady konstrukcyjne: powłokę z blachy falistej oraz zasypkę gruntową z nawierzchnią. Współdziałanie pomiędzy nimi modeluje się jako oddziaływanie kontaktowe, czyli siły o kierunku normalnym i stycznym do powierzchni powłoki. Oddziaływania te są zmienne w czasie budowy jak również podczas eksploatacji. W pracy podano dwa algorytmy wyznaczania sił kontaktowych. W pierwszym na podstawie odkształceń jednostkowych określa się siły wewnętrzne w powłoce a stąd oddziaływania kontaktowe. Do obliczeń niezbędna jest duża liczba punktów pomiarowych rozmieszczonych na paśmie obwodowym powłoki. W drugim algorytmie wykorzystuje się warunek kolokacji polegający na tym, że wynik obliczeń uzyskany z modelu geometrii powłoki ma być zgodny w rezultatem pomiaru przemieszczenia punktu kolokacyjnego obiektu. Gdy takich punktów jest więcej oszacowanie wyniku jest dokładniejsze. Zaletą obydwu algorytmów jest uwzględnienie cech fizycznych gruntu w warstwach zasypki a przede

wszystkim technologii jej układania i zagęszczania. Wyniki tych analiz mogą być podstawą do porównań skuteczności klasycznych modeli geotechnicznych.

Chociaż zależność między siłami kontaktowymi a deformacją powłoki jest znana, to procedury określenia oddziaływań kontaktowych na podstawie doświadczalnie wyznaczonych odkształceń czy też przemieszczeń powłoki nie są ściśle opisane. Celem pracy było przedstawienie takich procedur na przykładzie dwóch różnych obiektów gruntowo-powłokowych.

Podsumowanie uzyskanych wyników i ich analizy przedstawiono poniżej:

Korzystając z wyników pomiarów realizowanych na obiekcie (3D) sprowadza się zadanie do układu płaskiego (2D). Do określenia oddziaływań kontaktowych w postaci parcia p i sił stycznych t wykorzystuje się w pracy deformację powłoki określaną przez przemieszczenia punktów pomiarowych w postaci składowych pionowych w i poziomych u. Są one mierzone z zastosowaniem technik geodezyjnych – wystarczająco dokładnych z uwagi na duże wartości przemieszczeń. Oddziaływania kontaktowe można uzyskać również poprzez siły wewnętrzne w powłoce, które wyznacza się z deformacji powłoki ale określonej w wielu punktach pasma obwodowego z użyciem tensometrów a więc odkształceń jednostkowych. W tym sposobie pomiarowym realizuje się odmienną metologię badawczą.

Sprawdzeniem obydwu sposobów jest pomiar bezpośredni parcia gruntu uzyskiwany za pomocą presjometrów. Taki sposób pomiarowy jest bezpośrednią ingerencją w warstwę kontaktową pomiędzy ośrodek gruntowy i powłokę. W obydwu rozwiązaniach omawianych w pracy wykorzystuje się warunek zgodności oddziaływań kontaktowych pomiędzy gruntem a powłoką. Nie uwzględnia się zasady zgodności przemieszczeń czyli dopuszcza się powstawanie poślizgu w styku tych podukładów. Jest to ważną zaletą algorytmu.

Znajomość oddziaływań kontaktowych p i t umożliwia oddzielną analizę każdego z podukładów – niezależną powłokę z blachy falistej oraz zasypkę gruntową z nawierzchnią. Oddziaływania kontaktowe można wykorzystać do analizy sił wewnętrznych i przemieszczeń ośrodka gruntowego jako drugiego podukładu. Modelowanie gruntu jest trudne z uwagi na jego złożoną, warstwową budowę i indywidualne cechy fizyczne każdej warstwy. Określenie przemieszczeń gruntu na podstawie deformacja powłoki w warstwie kontaktowej jest bardzo trudne z uwagi na możliwość powstawania poślizgów w styku blachy i gruntu.

Zaletą obydwu przedstawionych algorytmów jest uwzględnienie cech fizycznych gruntu w warstwach zasypki a przede wszystkim technologii jej układania i zagęszczania. Analizuje się obiekty w fazie budowy a więc podczas układania zasypki gruntowej oraz użytkowania przy pełnym naziomie z nawierzchnią. W obliczeniach nie uwzględnia się udziału obciążeń pojazdami drogowymi lub kolejowymi. W obiektach gruntowo-powłokowych oddziaływania obciążeń ruchomych (zmieniających położenie) jest odrębnym zagadnieniem.

Analiza sił kontaktowych może być wykorzystana do modelowania warstwy kontaktowej w programach MES (PLAXIS, ABACUS). Model interfejsu powinien być jednak inny w fazie budowy (układanie zasypki), inny dla obciążeń użytkowych (przejazd pojazdów), a jeszcze inny do odwzorowania skutków eksploatacji (jako procesów długotrwałych). Szczególnie ważna jest obserwacja zmian oddziaływań p i t w trakcie eksploatacji. Do obserwacji tych zmian, przy wykorzystaniu sprzętu geodezyjnego z niewielką liczbą punktów pomiarowych, wykorzystywany może być algorytm drugi.

Dwa zaprezentowane algorytmy obserwacji zmian oddziaływań gruntu na powłokę mogą z powodzeniem zastąpić bardziej skomplikowane i droższe w realizacji pomiary z użyciem presjometrów.